OIL FILM PRESSURE OF JOURNAL BEARING WITH OIL SUPLY HOLE LOCATED IN THE HOUSING CONCERNING CAVITATION

ÁP SUẤT MÀNG DẦU Ổ TRƯỢT VỚI ĐƯỜNG CẤP DẦU TRÊN BẠC CÓ TÍNH ĐẾN SỰ XÂM THỰC

Tran Thi Thanh Hai*, Le Anh Dung, Dang Vu Vinh

ABSTRACT

During the operating, the lubricated oil film pressure of hydrodynamic bearing is varied under the load apply and under the rotation speed. This pressure is one important characteristic when studying the lubrication problem for the bearing. An experimental device and the journal bearing are used to determine the pressure and the temperature of the lubricated oil film. The load is applied on the housing bearing. The journal bearing is subjected to different applied load at different velocities. Lubricant oil is circulatingly supplied via oil supply hole in the housing. The oil film pressure is calculated by numerical modelization with Reynolds condition taking into account cavitation and also experimental measured by the pressure sensor with the same applied load. The calculated pressure and measured pressure of the oil film are agreement with the applied load. The calculated oil film pressure is corresponded to the measured pressure; however, the two types of results have a difference in value. As the load increase, the difference between the numerical modelization results and experimental results of maximum pressure increase significantly. When the rotation speed increases, the maximum pressure decreases, the minimum pressure in calculating increases and minimum pressure in experimenting is slightly varied.

Keywords: *Journal bearing, oil film pressure, cavitation, oil supply hole.*

TÓM TẮT

Trong quá trình làm việc, áp suất màng dầu bôi trơn của ổ thuỷ động thay đổi dưới tác dụng của tải trọng và tốc độ quay. Áp suất này là đặc tính quan trọng khi nghiên bài toán bôi trơn cho ổ. Một thiết bị thực nghiệm với một ổ đỡ thuỷ động được sử dụng để xác định áp suất và nhiệt độ màng dầu bôi trơn. Ổ đỡ chịu tải tác dụng và vận tốc khác nhau. Dầu bôi trơn được cấp tuần hoàn thông qua lỗ cấp dầu đặt trên bạc. Áp suất màng dầu tính toán mô phỏng với điều kiện biên Reynolds có tính đến sự xâm thực và thực nghiệm đo thông qua cảm biến áp suất với cùng tải tác dụng. Áp suất màng dầu tính toán tương đồng với áp suất thực nghiệm nhưng khác nhau về giá trị. Khi tăng tải, sự sai khác giữa áp suất lớn nhất tính toán và áp suất lớn nhất thực nghiệm tăng nhiều. Khi tốc độ quay tăng, áp suất lớn nhất giảm, áp suất nhỏ nhất khi tính mô phỏng giảm còn áp suất nhỏ nhất khi thực nghiệm thay đổi ít.

Từ khóa: *Ổ trượt, áp suất màng dầu, xâm thực, lỗ cấp dầu.*

School of Mechanical Engineering, Hanoi University of Science and Technology
*Email: hai.tranthithanh@hust.edu.vn
Received: 10 May 2020
Revised: 20 June 2020
Accepted: 24 June 2020

1. INTRODUCTION

The lubricated oil film pressure of hydrodynamic bearing is varied during the operating under the static or dynamic load. Hydrodynamic journal bearing based on hydrodynamic lubrication, which can be described as the load-carrying surfaces of the bearing are absolutely separated by a thin film of lubricant in order to prevent metal-to-metal contact. In 1991, Pai and Majumdar [1] analyzed the stability characteristics of submerged plain journal bearings under a unidirectional constant load and variable rotating load. In 1999, Raghunandana and Majumdar [2] analyzed the effects of non-Newtonian lubricant on the stability of oil film journal bearings under a unidirectional constant load. In 2000, Kakoty and Majumdar [3] analyzed the stability of journal bearings under the effects of fluid Inertia, the next year, Jack and Stephen [4] reviewed the theory of finite element applied on elasto-hydrodynamic lubrication. In 2012, Salmial et al. studied the experimental pressure distribution around the circumference of a journal bearing and experimental fluid frictional force of the bearing cause by shearing action. The results were compared to predicted values from established Raimondi and Boyd charts. The maximum pressure value is higher than the theoretical maximum pressure value. Fiction coefficients of oil lubricant decrease when the load increases. In 2019, Tran Thi Thanh Hai [6] presented a solution for measuring the oil film pressure of the connecting-rod big end bearing. The housing carries the pressure sensor and can rotate 15 degrees to measure the oil film pressure at the 24 different positons of bearing with the crank angle. 2020, Le Anh Dung et al. [7] simulated the equilibrium position of hydrodynamic bearing by using finite element method to solve Reynold equation in static load condition. The results show that, the more loads applied, the distance from the calculated equilibrium position to the journal center gets farther. Within the increase of the Sommerfeld number values, the equilibrium position moves closer to the *y*-axis. The faster journal rotation speed makes the balance point closer to the journal center.

In this study, we present the numerical modelization and experimenting of oil film pressure in the journal bearing at the different working regimes. The oil film pressure is determined by numerical modelization with Reynolds

condition taking into account cavitation and also measured by the pressure sensors with the same applied load.

2. NUMERICAL MODELIZATION

2.1. Journal bearing and the equations

The lubrication problem of the hydrodynamic bearing is solved based on solving the Reynolds equation, the oil film thickness equation at the dynamic regime. Fig. 1 is the middle section according to the length of the bearing. The load W is applied on the housing bearing. Oil supply hole is located on the housing and at the angle 45° respected to the load direction. At the symmetric position is the oil return hole. The diameter of these holes is 5mm.

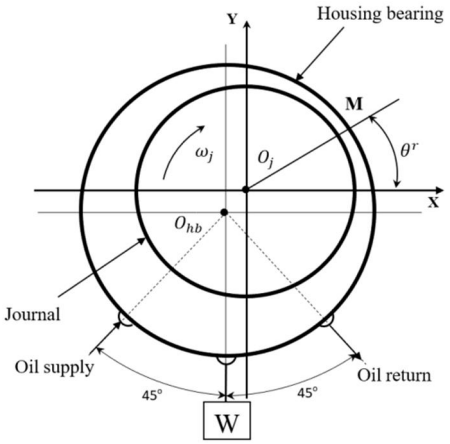

Figure 1. Plane section of bearing

The Reynolds equation is [8]:

$$\frac{\partial}{\partial x}\left(h^3\frac{\partial p}{\partial x}\right)+\frac{\partial}{\partial z}\left(h^3\frac{\partial p}{\partial z}\right)=6\mu v\frac{\partial h}{\partial x} \quad (1)$$

where: p is the oil film pressure, h is the oil film thickness, v is the velocity of journal, μ is the dynamic viscosity of lubricated oil, x and z are circumference and bearing length direction.

The boundary conditions used to solve the Reynolds equation are based on the separation of the active zone Ω and inactive zone (cavitation zone) Ω_o. In the active zone, the pressure is established and equilibrated with the applied load. In the inactive zone, the pressure (p_{cav}) is lower than the atmospheric pressure. The Figure 2 presents the active zone and inactive zone in the film domain.

- Active zone: $p > p_{cav}$
- Inactive zone: $p = p_{cav}$; $p_{cav} < 0$

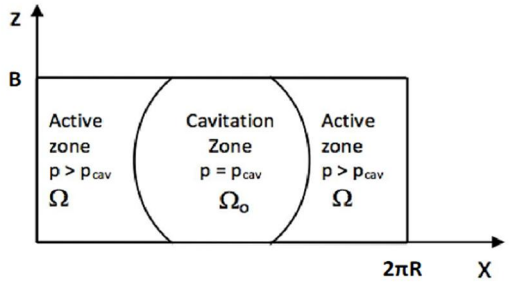

Figure 2. The active zone and the inactive zone in the film domain

With the dimensionless parameters:

$$\theta=\frac{x}{R};\ \zeta=\frac{z}{R};\ H=\frac{h}{C};P=\frac{p}{6\mu\omega\left(\frac{R}{C}\right)^2}$$

where: R is the radius of bearing, C is the radial clearance, ω is the angular velocity.

We obtained the dimensionless Reynolds equation:

$$\frac{\partial}{\partial\theta}\left(H^3\frac{\partial P}{\partial\theta}\right)+\frac{\partial}{\partial\zeta}\left(H^3\frac{\partial P}{\partial\zeta}\right)=\frac{\partial H}{\partial\theta} \quad (2)$$

The film thickness equation:

$H(\theta')=1-\varepsilon_x\cos\theta-\varepsilon_y\sin\theta$; ε is the eccentricity ratio. (3)

The forces acting on the oil film is represented by the following formula:

$$f=\begin{Bmatrix}F_x(\bar{x},\bar{y})\\F_y(\bar{x},\bar{y})\end{Bmatrix}=\sum_{\Omega}\begin{Bmatrix}\iint_{\Omega}-P.\cos\theta d\theta d\zeta\\\iint_{\Omega}-P.\sin\theta d\theta d\zeta\end{Bmatrix}=\begin{Bmatrix}w_x\\w_y\end{Bmatrix}=w \quad (4)$$

with $\bar{u}=(\bar{x},\bar{y})$ is the vector (ε_x, ε_y), f is the vector of the hydrodynamic force, w is the vector of the external force, F_x, F_y, w_x and w_y are respectively the hydrodynamic force and external force along x and y axis.

2.2. Discretization of the Reynolds Equation

The film is discretized by quadrangular elements with four nodes (Figure 3).

The pressure at the point in the element is calculated:

$$P=\sum_{i=1}^{n}P_iN_i=P^T\{N_i\} \quad (5)$$

with N is the shape function.

Figure 3. Solid surface mesh

Thus $\partial P_e=\partial N_i\{P_i\}$ and the left side of the (2) is written as:

$$VT=\{M_e\}=\iint_{S_e}\frac{\partial\{N_i\}}{\partial\theta}H_e^3\frac{\partial N_i}{\partial\theta}\{P_i\}d\theta d\zeta+$$

$$+\iint_{S_e}H_e^3\frac{\partial\{N_i\}}{\partial\zeta}\frac{\partial N_i}{\partial\zeta}\{P_i\}d\theta d\zeta$$

where "e" is representative for each element.

The right side of the (2) is:

$$VP=\{B_e\}=-\iint_{S_e}\{N_i\}.\frac{\partial H_e}{\partial\theta}dS_e$$

Assemble the elements we obtain the equation for the whole mesh:

$$M.P = -B \quad (6)$$

where *M* is stiffness matrix and *B* is the "load vector".

By solving (3), we obtain the pressure for the oil film.

2.3. Discretization of the Equilibrium of the Charge

Substitution (5) into the left-side of (4), we have:

$$f = \begin{Bmatrix} F_x(\bar{x},\bar{y}) \\ F_y(\bar{x},\bar{y}) \end{Bmatrix} = \sum_{\Omega} - \begin{Bmatrix} P^T \iint_{\Omega} N.\cos\theta d\theta d\zeta \\ P^T \iint_{\Omega} N.\sin\theta d\theta d\zeta \end{Bmatrix} \quad (7)$$

In the formula (7), we take:

$$S = \iint_{\Omega} N.\cos\theta d\theta d\zeta; R = \iint_{\Omega} N.\sin\theta d\theta d\zeta \quad (8)$$

Jacobian matrix of the force vector:

$$J_{\bar{u}}\bar{f}(\bar{u}) = \begin{bmatrix} \frac{\partial F_x(\bar{x},\bar{y})}{\partial\bar{x}} & \frac{\partial F_x(\bar{x},\bar{y})}{\partial\bar{y}} \\ \frac{\partial F_y(\bar{x},\bar{y})}{\partial\bar{x}} & \frac{\partial F_y(\bar{x},\bar{y})}{\partial\bar{y}} \end{bmatrix} \quad (9)$$

where x and y are the coordinate axis located on journal center according to Figure 1.

Replace (8) into (9), we get:

$$J_{\bar{u}}\bar{f}(\bar{u}) = -\begin{Bmatrix} S^T \\ R^T \end{Bmatrix} \begin{bmatrix} P_{\bar{x}} & P_{\bar{y}} \end{bmatrix} = -\begin{bmatrix} S^T P_{\bar{x}} & S^T P_{\bar{y}} \\ R^T P_{\bar{x}} & R^T P_{\bar{y}} \end{bmatrix}$$

where $P_{\bar{x}} = \frac{\partial P}{\partial\bar{x}}; P_{\bar{y}} = \frac{\partial P}{\partial\bar{y}}$

Rewrite (3) as:

$$M(\bar{x},\bar{y})P = -B(\bar{x},\bar{y}) \quad (10)$$

Derivative (9) respect to the components $\bar{x},\bar{y}$ we obtain:

$$M\left[P_{\bar{x}}, P_{\bar{y}}\right] = \left[-M_{\bar{x}}P + B_{\bar{x}}, -M_{\bar{y}}P + B_{\bar{y}}\right] \quad (11)$$

where $M_{\bar{x}} = \frac{\partial M}{\partial\bar{x}}, M_{\bar{y}} = \frac{\partial M}{\partial\bar{y}}; B_{\bar{x}} = \frac{\partial B}{\partial\bar{x}}; B_{\bar{y}} = \frac{\partial B}{\partial\bar{y}}$

$$\begin{cases} \frac{\partial B_i}{\partial\bar{x}} = \iint_{\Omega} N_i \sin\theta d\theta d\zeta, \frac{\partial B_i}{\partial\bar{y}} = -\iint_{\Omega} N_i \cos\theta d\theta d\zeta \\ \frac{\partial M_{ij}}{\partial\bar{x}} = \iint_{\Omega} H^2 \cos\theta \left(\frac{\partial N_i}{\partial\theta}\frac{\partial N_j}{\partial\theta} + \frac{\partial N_i}{\partial\zeta}\frac{\partial N_j}{\partial\zeta} \right) d\theta d\zeta \\ \frac{\partial M_{ij}}{\partial\bar{y}} = \iint_{\Omega} H^2 \sin\theta \left(\frac{\partial N_i}{\partial\theta}\frac{\partial N_j}{\partial\theta} + \frac{\partial N_i}{\partial\zeta}\frac{\partial N_j}{\partial\zeta} \right) d\theta d\zeta \end{cases} \quad (12)$$

Solving the system of (11), we get the vector $(P_{\bar{x}}, P_{\bar{y}})$. Substitute it into (9) to obtain the Jacobi matrix $J_{\bar{u}}\bar{f}(\bar{u})$. Then the vector $\bar{u} = (\bar{x},\bar{y})$ is calculated from the interpolation steps according to the following formula:

$$\bar{u}^{(k+1)} = \bar{u}^{(k)} - J_{\bar{u}}^{-1}\bar{f}(\bar{u})\left[f(\bar{u}^{(k)}) - w \right] \quad (13)$$

3. EXPERIMENTAL MEASURMENT OF OIL FILM PRESSURE

3.1. Experimental device

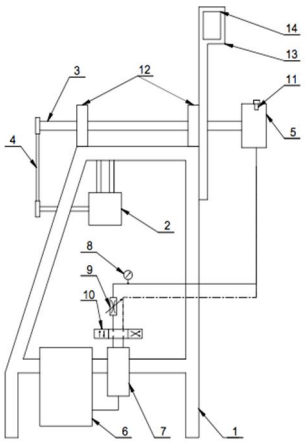

Figure 4. Functional scheme and photography of experimental device

The experimental device used in this study respects the kinematics of bearing, including a shaft and a housing. The photography and functional scheme of the experimental device are presented on Figure 4. An electric motor (2) with transmits motion to the shaft (3) through the belt (4). The shaft is supported by two pillow blocks (5). The shaft, the housing bearing (6) and the oil film created when the shaft rotates together form the journal bearing in this study. The pressure sensors (12) are attached on the bearing to capture the real pressure in time at the different positions along the perimeter of the middle section of the bearing. The oil feed hydraulic system which consists of the oil tank (7), the oil pump (8), the directional controlling valve (9), the flow control valve (10), the pressure gauge (11), oil feed pipe and oil return pipe. However, the housing bearing can slightly rotate within rotating direction of the journal.

This experimental device is used to research lubricated condition of hydrodynamic bearing at different operating regimes. Electric motor power is 0.55kW, rotational speed is 1390rpm and driven by an inverter. Belt transmission ratio is 1/2, so that rotation speed range of studied bearing is from 0 to 695rpm. Position of two pulleys are interchangeable to make the ratio becomes 2, which means the rotation speed range is 0 to 2780rpm. Load is apply on the housing by hanging weights.

The dimensions of the bearing as follows: length of the bearing L= 50mm, diameter of the bearing D = 70mm, precision of the shaft surface is up to 8 level, precision of the housing up to 6 level, the radial clearance C = 0.05mm; lubricated oil with viscosity μ = 0.015Pa.s; the density ρ = 850kg/m^3.

The Figure 5 shows the studied journal bearing. The part of the shaft, which its diameter D and length L, play the role as the journal of the journal bearing. During operation, the journal center is supposed to be unmoved and the housing

center position is changed which makes the distance between these two centers varies depend on the value of applied load. The lubricated oil film pressure is measured at five different positions A1, A2 A3, A4, A5 on the middle cross-section in the middle of the bearing according to the perimeter by five pressure sensors (Fig.6) [9].

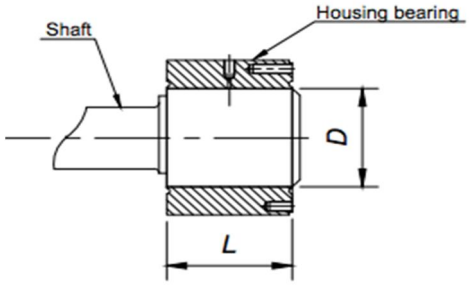

Figure 5. Journal bearing study

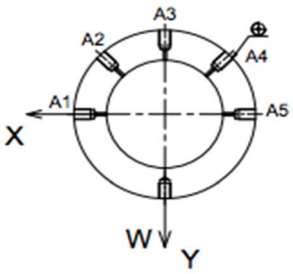

Figure 6. Pressure sensor location

3.2. Experimental method

The pressure of the oil film is measured at different working regimes with the loads 140N, 170N, 200N and velocities 200rpm, 400rpm, 600rpm. After starting the experimental device for 10 minutes, the first measurement is read, and after that the break time between measurements is 15 minutes. For each load level or velocity, the measurements were recorded eight times. The measurement results were analysed by using technique for analysis of experimental data by Minitab software.

4. THE RESULTS

With the algorithm presented in part 2, we program on Fortran software. The lubricated oil film pressure of the journal bearing is calculated and also measured with the same applied load. The table 1 presents the oil film measurement pressure at different loads and at different rotational frequencies. These pressure values are obtained by the experimental data process. Five pressure value p_1, p_2, p_3, p_4, p_5 are the oil film pressure at five positions A1, A2, A3, A4, A5.

Table 1. Measured oil film pressure at different load and at different velocities

Load (N)	Velocity (rpm)	Oil film pressure at positions A1, A2 A3, A4, A5 (KPa)				
		p_1	p_2	p_3	P_4	P_5
140	300	7.58	41.13	64.69	63.05	15.5
	400	8.12	43.41	61.53	61.93	17.2
	600	6.98	40.02	57.74	58.78	16.61
170	300	9.16	42.37	73.66	77.1	13.36
	400	8.42	41.62	71.50	74.31	14.57
	600	7.51	39. 34	72.08	70.16	15.32
200	300	12.41	47.19	88.17	85.50	16.79
	400	11.08	52.51	82.50	84.62	18.22
	600	9.54	54.03	85.58	82.90	19.39

Fig. 7 shows the numerical modelization pressures at the middle cross-section in the middle of the bearing according to the perimeter, the load of 200N and the velocities of 300rpm, 400rpm and 600rpm. It shows that, the pressure is positive in the charge zone, from 0° to 210° of the housing bearing. When the rotation speed increases, the maximum value pressure is decreases and the zone pressure is larger. It can be explained that the minimum film thickness increases when the velocities increase.

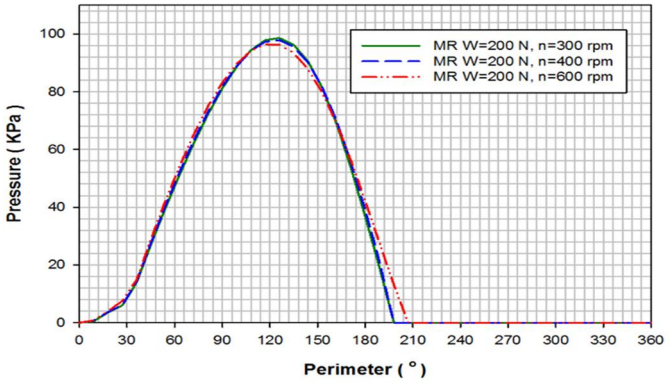

Figure 7. Calculated pressure (MR) at the different rotation speeds, load W = 200N

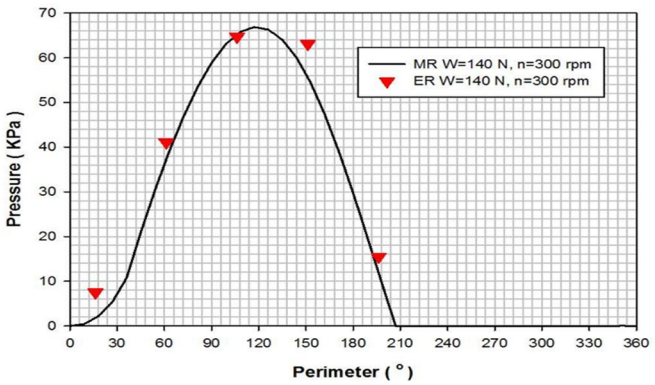

Figure 8. Comparision the oil film pressurebetween the calculated results (MR) and measured results (ER) at the load W = 140N, 300rpm

Figure 8 represents a comparison between numerical modelization pressure and measured in experiments at the load of 140N and velocity of 300rpm. When the bearing works, the bearing housing rotates an angle from the original. It means, the sensor positions also rotate an angle with the housing bearing. We note, the good agreement on the film pressure. However, the maximum pressure in the calculated is 66.5kPa at 117° of boring, the maximum in experiment is 64.69kPa at the 105°. That can be explained, the maximum pressure position of oil film is not the same as the position of

pressure sensor. It means, the pressure reaches the maximum value at a position in the range from A3 to A4. The real maximum value of pressure is not measured.

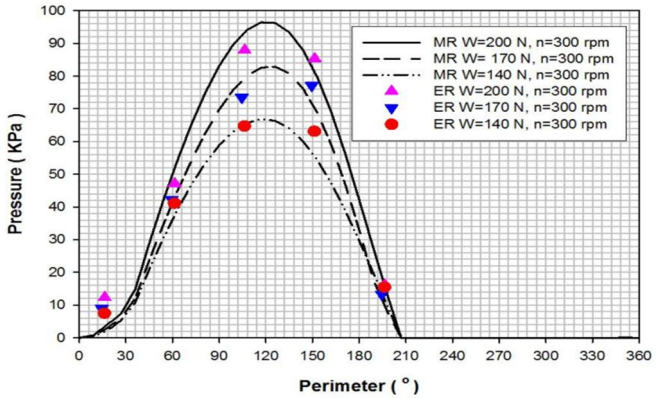

Figure 9. Comparision oil film pressure between the calculated results (MR) and measured results (ER) at the different load applied, 300rpm

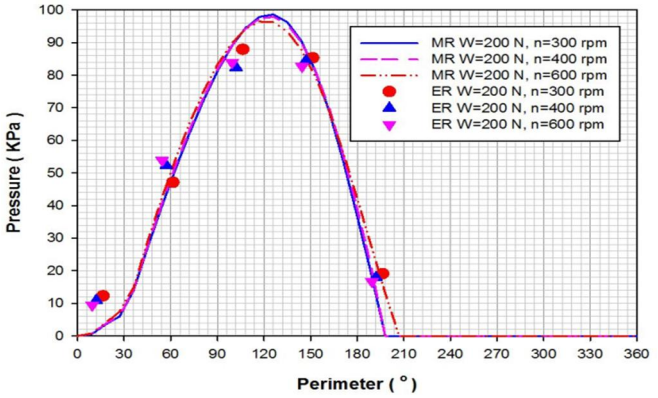

Figure 10. Comparision the oil film pressure between the calculated results (MR) and measured results (ER) at the load W = 200N,300rpm

Fig. 9 shows a comparison of oil film pressure in calculation and in experiment at different applied loads and journal speed of 300rpm. It shows that, the more load applied, the greater difference in in maximum value between the of calculated pressure and measured pressure. At the loads of 140N, 170N and 200N, the maximum pressure of experiment is corresponding to 64.69kPa, 77.1kPa, 88.17kPa and the numerical result is 65.5kPa, 83.25kPa, 96.03kPa. Thus, it remains to suppose that the experimental device has an imperfection of operation which is not considered the numerical simulation. The minimum pressure is slightly varied.

Fig. 10 represents a comparison between the oil film pressure in numerical simulation and measured at the different rotational frequencies for the load applied of 200N. The maximum pressure values decrease when the velocity increases. However, the decrease in maximum calculated pressure value is less than the decrease in experimental value. At the rotational frequencies of 300rpm, 400rpm, 600rpm, the maximum calculated pressures are corresponding to 98.63kPa, 97.2kPa, 96.01kPa and the experimental results are 88,17kPa, 84.62 KPa, 85.58 KPa respectively. The minimum pressure is slightly varied.

5. CONCLUSION

This research presents the numerical modelization pressure and the experimental pressure of the lubricated oil film for the journal bearings with circulating oils. Lubricant oil is supplied via oil supply hole in the housing. The pressure is calculated based on solving the Reynolds equation taking into account cavitation condition and the oil film thickness equation, and the equilibrium of the charge equation which are discretized by a finite element mesh and are solved by using Newton-Raphson iterations. The measured pressure of the oil film is determined at five different positions on the cross-section in the middle of the bearing according to the perimeter by pressure sensors.

The results show the good agreement on the film pressures. The pressure is positive in the charge zone, from 0° to around 210° of the housing bearing. However, the more load applied, the greater difference in value between the maximum of calculated pressure and measured pressure. Thus, it remains to suppose that the experimental device has an imperfection of operation which is not considered in the numerical simulation. The minimum pressure is slightly varied.

The maximum pressures decrease when the velocity increases and the pressure zone is larger. However, the decrease in experimental pressure is more than the decrease in calculated pressure. The minimum pressure is slightly varied.

REFERENCES

[1]. Pai R., B.C. Majumdar, 1991. *Stability analysis of flexible supported rough submerged oil journal bearings*. Tribol. T., 40(3), 437-444.

[2]. Raghunandana K., Majumdar B. C., 1999. *Stability of Journal Bearing Systems Using Non-Newtonian Lubricants: A Non-Linear Transient Analysis*. Tribol. Int., 32, pp. 179-184.

[3]. Kakoty S.K., B.C. Majumdar, 2000. *Effect of fluid inertia on stability of oil journal bearings*. ASME J. Tribol., 122, 741-745.

[4]. Salmiah K, Mohamad Ali Ahmad, Rob-Dwyer Joyce, Che Faridah Mat Taib, 2012. *Preliminary study of Pressure Profile in Hydrodynamic Lubrication.* Journal Bearing. Procedia Engineering 41 (2012), 1743-1749.

[5]. Tran Thi Thanh Hai, 2018. *A solution for measuring the oil film pressure of the connecting-rod big end bearing in the experimental device*. Journal of Science and Technology-The University of Danang, No. 11(132).2018, Vol. 1, pp 22-25.

[6]. Le Anh Dung, Tran Thi Thanh Hai, Luu Trong Thuan, 2020. *Numerical modelization for equilibrium position of a static loaded hydrodynamic bearing*. Journal of Science and Technology Technical university, No.141 (2020), pp 28-33.

[7]. Bonneau D., Fatu A., Shouchet D., 2014. *Hydrodynamic Bearings*. ISTE, London and John Wiley & Sons, New York.

[8]. Pham Trung Thien, Tran Thi Thanh Hai, 2016. *Development a supervise system of pressure and temperature for journal bearing*. Master thesis, Hanoi University of Science and Technology.

THÔNG TIN TÁC GIẢ

Trần Thị Thanh Hải, Lê Anh Dũng, Đặng Vũ Vinh

Viện Cơ khí, Trường Đại học Bách khoa Hà Nội